Supporting information

A. The most stable TM-intercalated BLG sandwich with the coverage of $x = 1$

As shown in Fig. S1, for Sc, the most stable intercalated site is AA-H site under the strain of 6%. For Ti and V, the most stable intercalated site is AB-TT site under the strains of 4% and 3%, respectively. Although the isolated Sc atom is bigger than isolated Ti atom, the $D_{G\text{-}G}$ of C_2TiC_2 is much bigger than that of C_2ScC_2. For Co and Ni, the most stable intercalated site is the center site of crossed C-C bonds in malposed BLG under the strain of 2%. For Fe, the most stable intercalated site is AA-T site under the strain of 2%. Fe is reported to prefers being at the same site with Co and Ni when intercalating BLG (c.f. Fig. S1(d)).[1] We compared the total energies of the two configurations of Fe-intercalated BLG, and the energy difference is 0.18 eV. For V, Co, and Ni, our results are in line with the previous ones of previous theoretical study.[1]

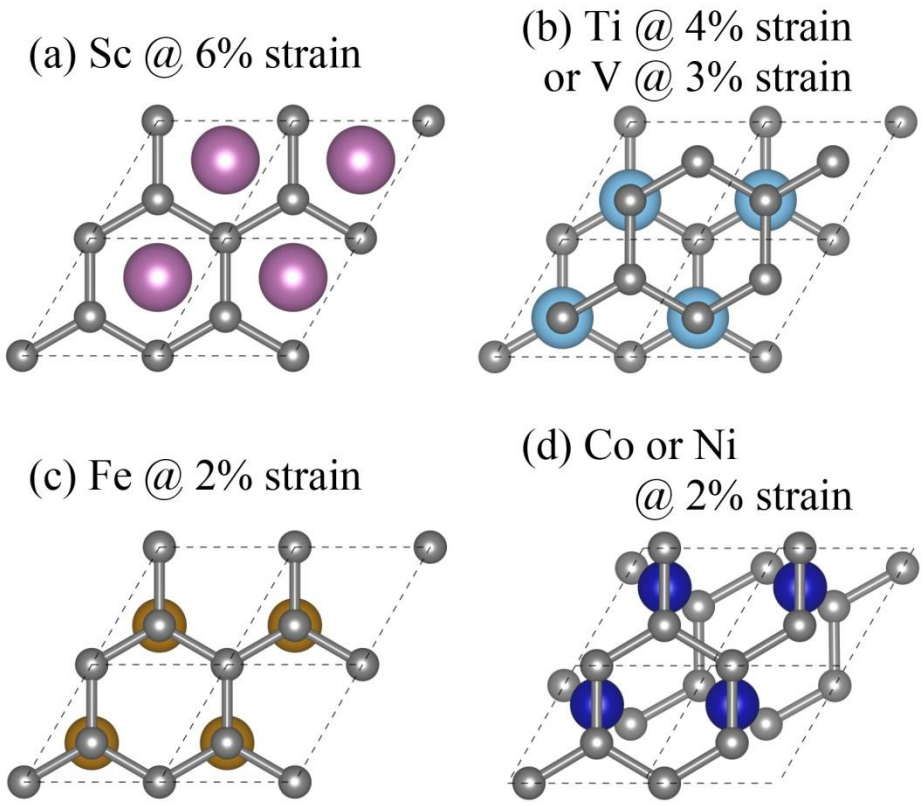

Fig. S1 Top view of the most stable structures of the (a) Sc-, (b) Ti- or V-, (c) Fe-, and (d) Co- or Ni-intercalated BLG sandwich at $x = 1$. Atoms are represented as follows: small gray ball for C; purple ball for Sc; light blue ball for Ti or V; dark yellow ball for Fe; blue ball for Co or Ni.

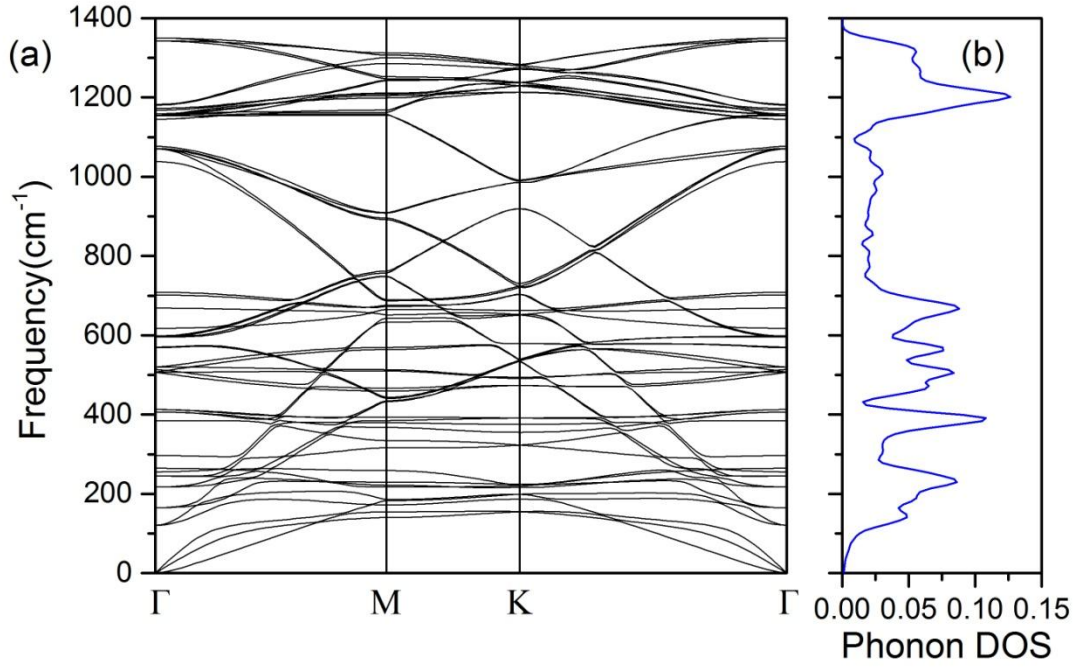

Fig. S2 DFPT calculated (a) phonon dispersion and (b) phonon density of states of $C_8Ti_3C_8$ at 5% biaxial strain.

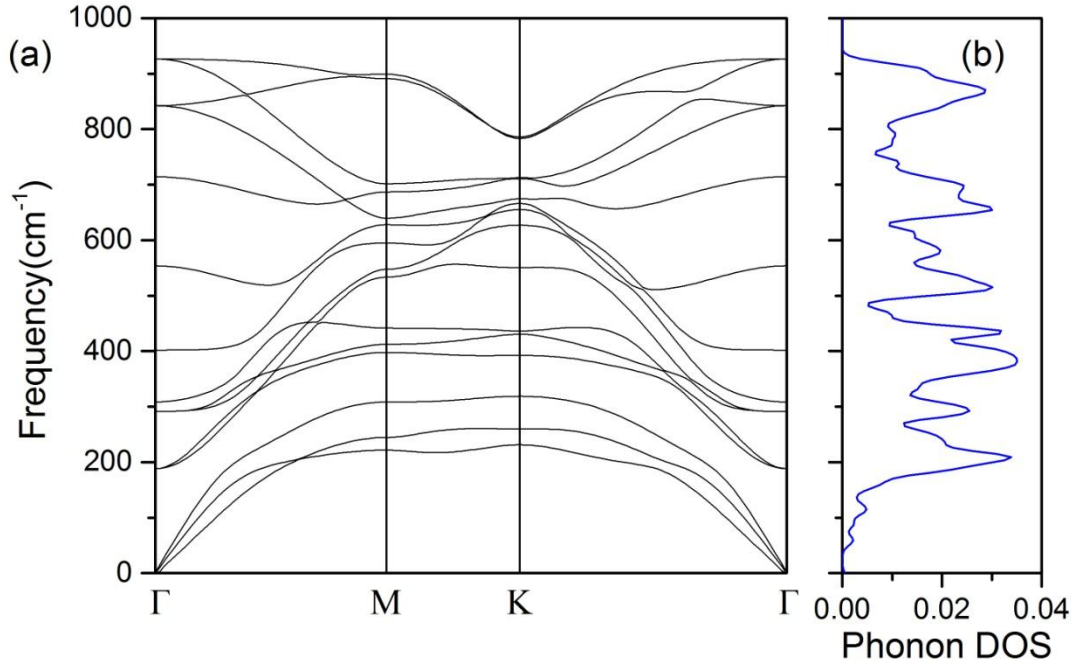

Fig. S3 DFPT calculated (a) phonon dispersion and (b) phonon density of states of C_2TiC_2 at 15% biaxial strain.

Table S1 The distance, $d_{m\text{-}m}$, between two nearest atoms, the interaction energy, E_i, of closely packed *3d* metal sheet, the adsorption energy, E_b, of *3d* TM atoms on 4×4 graphene, the binding energy, $E_{b\text{-BLG}}$, of *3d* TM atoms in 4×4 BLG, and the ratios of $(E_i+E_b)/E_c$ and $(E_i+E_{b\text{-BLG}})/E_c$.

	$d_{m\text{-}m}$(Å)	E_i(eV)	E_b(eV)	$E_{b\text{-BLG}}$(eV)	E_c(eV)	$(E_i+E_b)/E_c$	$(E_i+E_{b\text{-BLG}})/E_c$
Sc	3.13	2.66	1.36	2.73	3.90	**1.03**	**1.38**
Ti	2.66	3.43	1.66	3.23	4.85	**1.05**	**1.37**
V	2.46	3.37	1.16	2.64	5.31	0.85	**1.13**
Cr	2.35	1.77	0.30	0.64	4.10	0.51	0.59
Mn	2.70	1.98	0.20	0.48	2.92	0.75	0.84
Fe	2.42	3.34	0.73	1.48	4.28	0.95	**1.12**
Co	2.35	3.73	1.16	1.80	4.39	**1.11**	**1.26**
Ni	2.37	3.79	1.67	2.32	4.44	**1.23**	**1.38**
Cu	2.46	2.78	0.30	0.62	3.49	0.88	0.97
Zn	2.53	0.79	0.00	-0.13	1.35	0.59	0.49

Table S2 Total energies, E_{tot}, of C_2TMC_2 with various configurations under the strains ranging from 0% to 15%, and the distance between upper graphene and lower graphene $D_{G\text{-}G}$ of the most stable configuration at given strain.

		E_{tot}(eV) AA stacking				E_{tot}(eV) AB Stacking				
TM	Strain	H	T	B	X	TH	TT	BB	BX	$D_{G\text{-}G}$(Å)
Sc	0%	**-41.71**	-41.43	-41.35	*to H*	-41.54	-41.48	*to TH*	*to TH*	4.13
	5%	**-42.48**	-41.88	-41.80	*to H*	-42.17	-41.91	*to TH*	*to TH*	4.02
	6%	**-42.49**	-41.83	-41.75	*to H*	-42.15	-41.86	*to TH*	*to TH*	4.00
	7%	**-42.45**	-41.74	-41.65	*to H*	-42.10	-41.77	*to TH*	*to TH*	3.98
	10%	**-42.10**	-41.26	-41.14	*to H*	-41.75	-41.29	*to TH*	*to TH*	3.93
	15%	**-40.94**	-39.96	-39.74	*to H*	-40.60	-39.99	*to TH*	*to TH*	3.83
Ti	0%	-43.59	-43.86	-43.69	*to T*	-43.79	**-43.97**	*to TH*	*to TT*	4.44
	3%	-44.09	-44.17	-43.96	*to T*	-44.22	**-44.28**	*to TH*	*to TT*	4.36
	4%	-44.15	-44.17	-43.95	*to T*	-44.27	**-44.29**	*to TH*	*to TT*	4.34
	5%	-44.14	-44.13	-43.90	*to T*	**-44.27**	-44.24	*to TH*	*to TH*	3.99
	10%	-43.54	-43.37	-43.03	*to T*	**-43.72**	-43.46	*to TH*	*to TH*	3.83
	15%	-42.14	-41.91	-41.42	*to T*	**-42.43**	-41.99	*to TH*	*to TH*	3.74
V	0%	-44.41	-45.23	-44.88	*to T*	-45.00	**-45.27**	*to TT*	*to TT*	4.22
	2%	-44.71	-45.43	-45.03	*to T*	-45.26	**-45.47**	*to TT*	*to TT*	4.17
	3%	-44.76	-45.44	-45.02	*to T*	-45.30	**-45.49**	*to TT*	*to TT*	4.15
	4%	-44.76	-45.41	-44.96	*to T*	-45.30	**-45.45**	*to TT*	*to TT*	4.13
	5%	-44.71	-45.33	-44.86	*to T*	-45.24	**-45.37**	*to TT*	*to TT*	4.11
	10%	-43.82	-44.36	-43.75	*to T*	-44.35	**-44.39**	*to TT*	*to TT*	4.01
	15%	-42.18	-42.67	-41.98	*to T*	-42.69	**-42.71**	*to TT*	*to TT*	3.95
Fe	0%	-44.19	**-44.56**	-44.35	*to T*	-44.21	-44.46	*to TT*	*to TT*	4.13
	1%	-44.17	**-44.64**	-44.43	*to T*	-43.95	-44.54	*to TT*	*to TT*	4.12
	2%	-44.09	**-44.67**	-44.45	*to T*	-43.97	-44.57	*to TT*	*to TT*	4.12
	3%	-43.33	**-44.64**	-44.42	*to T*	-43.94	-44.55	*to TT*	*to TT*	4.10
	5%	-43.14	**-44.44**	-44.22	*to T*	-43.75	-44.36	*to TT*	*to TT*	4.08
	10%	-42.01	**-43.27**	-43.16	*to T*	-42.62	-43.22	*to TT*	*to TT*	4.03
	15%	-40.23	-41.44	-41.48	**-41.55**	-40.89	-41.43	-41.51	*to BB*	3.83
Co	0%	-43.03	-43.34	-43.39	*to B*	-43.05	-43.28	-43.40	**-43.45**	3.92
	1%	-42.97	-43.45	-43.48	*to B*	-43.05	-43.36	-43.48	**-43.55**	3.90
	2%	-42.86	-43.47	-43.52	*to B*	-43.00	-43.37	-43.51	**-43.58**	3.89
	3%	-42.71	-43.43	-43.50	*to B*	-42.64	-43.33	-43.48	**-43.57**	3.88
	5%	-41.67	-43.22	-43.32	*to B*	-42.42	-43.13	-43.30	**-43.40**	3.86
	10%	-40.54	-42.00	-42.23	*to B*	-41.29	-41.95	-42.18	**-42.32**	3.81
	15%	-38.86	-40.15	-40.50	*to B*	-39.55	-40.12	-40.51	**-40.61**	3.77
Ni	0%	-41.76	-41.91	-41.86	*to T*	-41.66	-41.78	-41.91	**-41.92**	3.97
	1%	-41.71	-42.01	-41.97	-42.02	-41.63	-41.87	-42.02	**-42.02**	3.95
	2%	-41.60	-42.04	-42.02	-42.06	-41.62	-41.90	-42.06	**-42.07**	3.93
	3%	-41.34	-42.02	-42.02	-42.05	-41.32	-41.88	-42.05	**-42.06**	3.91
	5%	-41.00	-41.83	-41.87	-41.90	-41.11	-41.70	-41.89	**-41.92**	3.88
	10%	-39.25	-40.70	-40.87	-40.88	-39.98	-40.60	-40.88	**-40.90**	3.81
	15%	-37.46	-38.91	-39.21	-39.24	-38.24	-38.85	-39.24	**-39.26**	3.75

B. Nesting homogenously distributed metal sheet into BLG

For the hexagonal planar lattice, the primitive cell is marked with $a_1 = a_2,\ \varphi = 120°$, and the supercell with $a_1' = a_2',\ \varphi = 120°$, and then

$a_1'^2 = (u_1 a_1)^2 + (u_2 a_2)^2 + 2u_1 a_1 u_2 a_2 \cos\varphi = ({u_1}^2 + {u_2}^2 - u_1 u_2){a_1}^2 = u^2 {a_1}^2$,

where u_1 and u_2 are arbitrary integer, so the positive integer u^2 can be 1, 3, 4, 7, 9, 12, 13, 16, 19, 21, 25, etc. The u^2 can not be 2, 5, 6, 8, 11, 14, 15, 17, 18, 20, 22, 23, 24, etc. The homogenous distribution of metal sheet intercalated BLG can be realized with the coverage ratio n_1/n_2, where $n_1, n_2 \in u^2$. For example, we can get the configuration of $C_{18}M_7C_{18}$ with the metal atoms' uniform distribution through nesting a $\sqrt{7} \times \sqrt{7}$ supercell of hexagonal metal sheet to the 3×3 supercell of BLG.

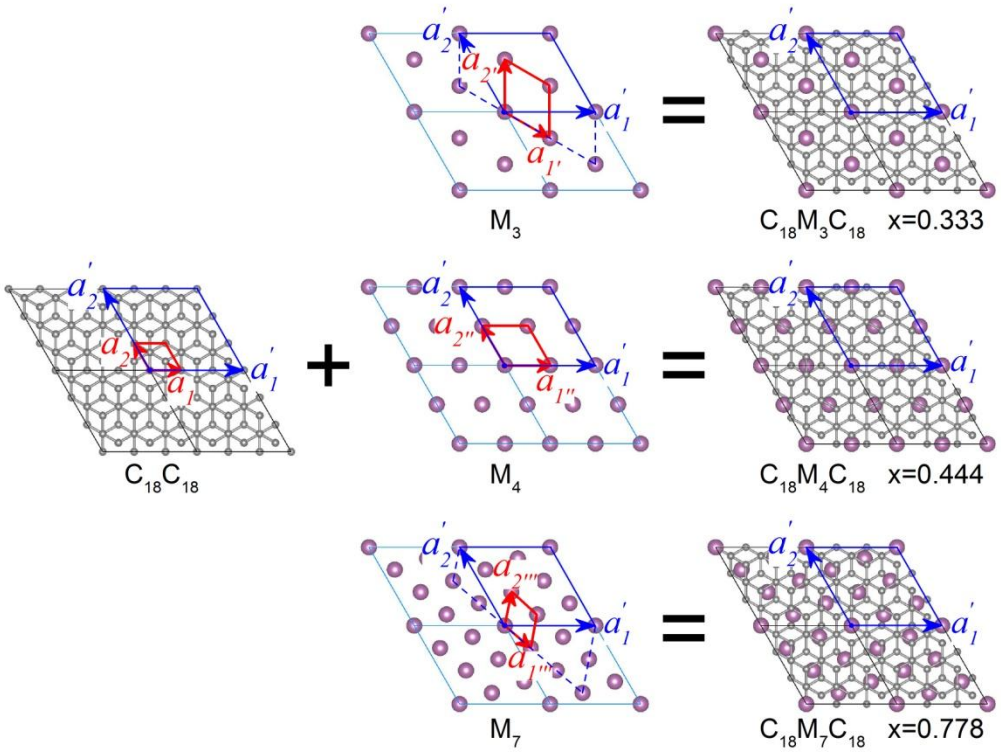

Fig. S4 Examples of nesting homogenously distributed metal sheet into AB stacking BLG. The primitive cells are shown in red rhombus. The first example is $C_{18}C_{18}$+M_3= $C_{18}M_3C_{18}$. For graphene, the supercell is 3×3 primitive cell, $a_1' = 3a_1, a_2' = 3a_2$. For metal sheet, the supercell is $\sqrt{3} \times \sqrt{3}$ primitive cell, $a_1' = 2a_{1'} + a_{2'}, a_2' = -a_{1'} + a_{2'}, |a_{1'}| = s|a_1|$, where s is scale factor. The second example is $C_{18}C_{18}$+M_4= $C_{18}M_4C_{18}$. For metal sheet, the supercell is 2×2 primitive cell. The last example is $C_{18}C_{18}$+M_7= $C_{18}M_7C_{18}$. For metal sheet, the supercell is $\sqrt{7} \times \sqrt{7}$ primitive cell, $a_1' = 3a_{1'''} + 2a_{2'''}, a_2' = -2a_{1'''} + a_{2'''}$.

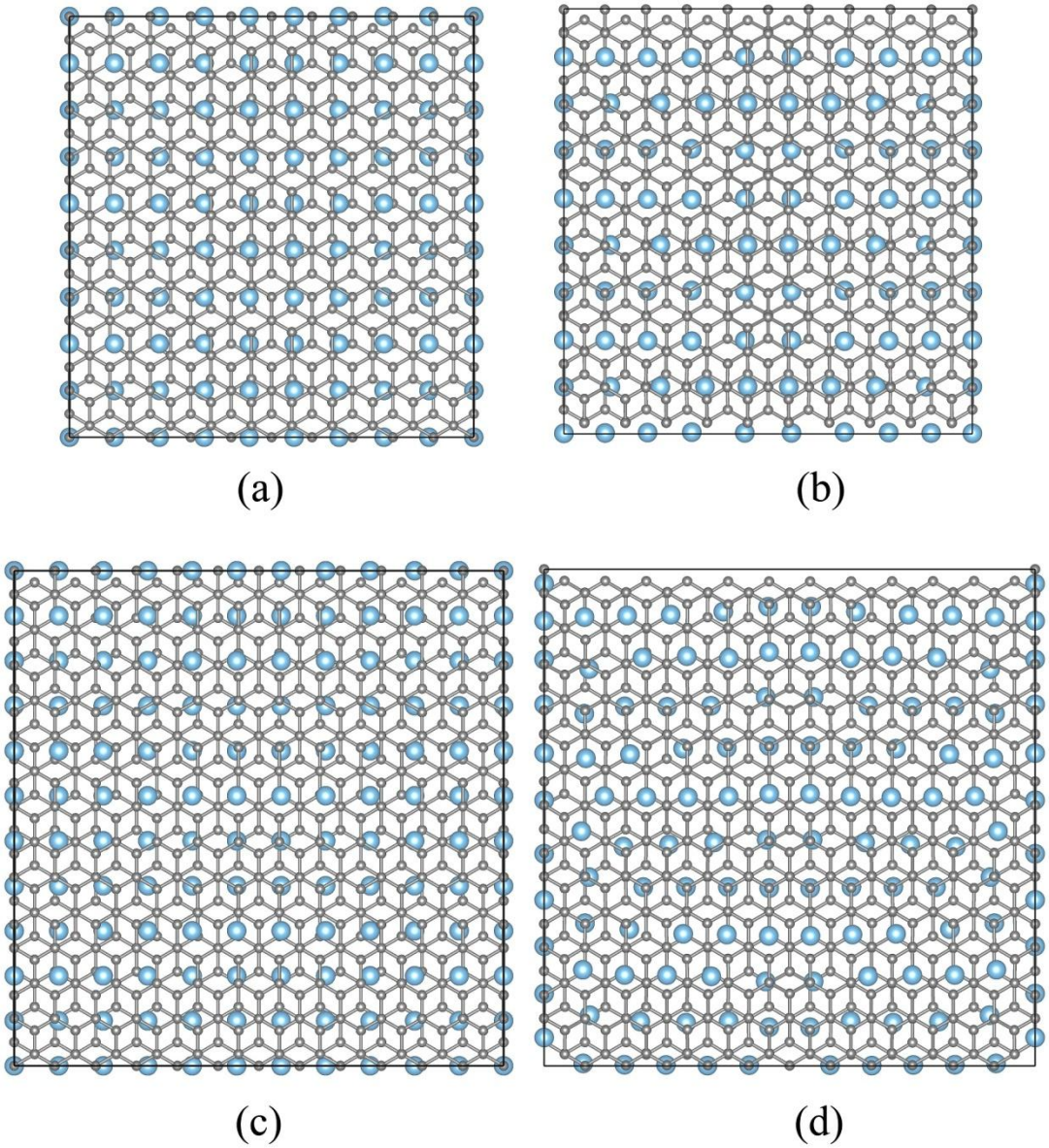

Fig. S5 Top view of the (a) initial and (b) relaxed configurations of the $C_{240}Ti_{81}C_{240}$ with $x = 0.675$ and (c) initial and (d) relaxed configurations of the $C_{336}Ti_{121}C_{336}$ with $x = 0.720$.

C. Magnetic configurations of $C_8Ti_3C_8$

Two stable magnetic configurations (i.e., FM and AFM coupling structures) are considered. The energy difference, $\Delta E = E_{\mathrm{FM}} - E_{\mathrm{AFM}}$, per unit of $C_8Ti_3C_8$ as a function of strain is presented in Fig. S6. Based on the DFT calculations, almost all of the magnetic moment comes from the Ti atoms at the TT sites. Therefore, we considered the coupling of the Ti atoms at the TT sties. An AFM coupling is shown in Fig. S6. Another AFM coupling, where the upper two Ti atoms at TT sites exchanged their spin direction, is equivalent due to the symmetry. The FM coupling configuration is the ground state.

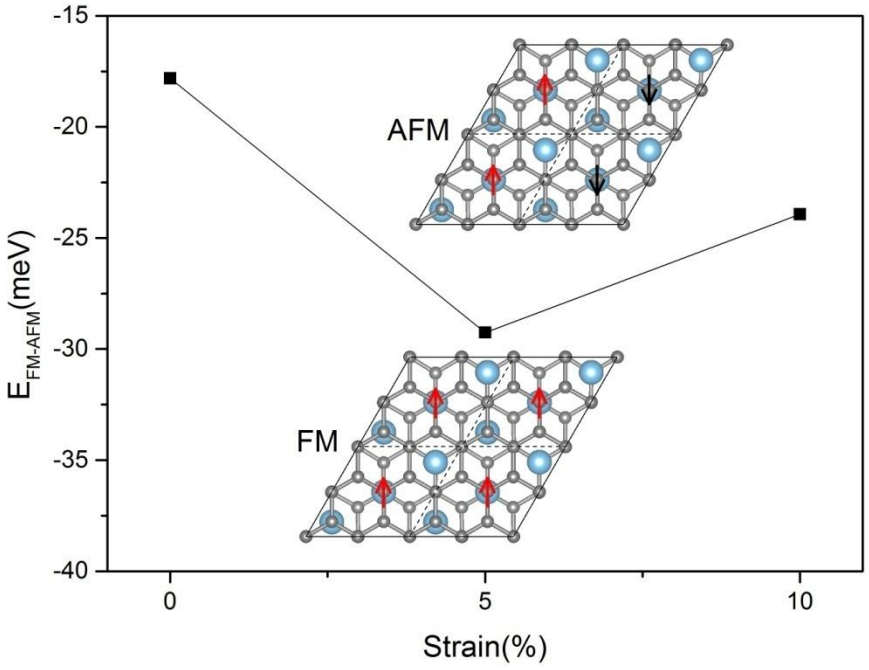

Fig. S6 Dependence of the energy difference on biaxial strain per unit ($C_8Ti_3C_8$) between FM and AFM coupling. The insets give the schematic illustrations of AFM and FM couplings.

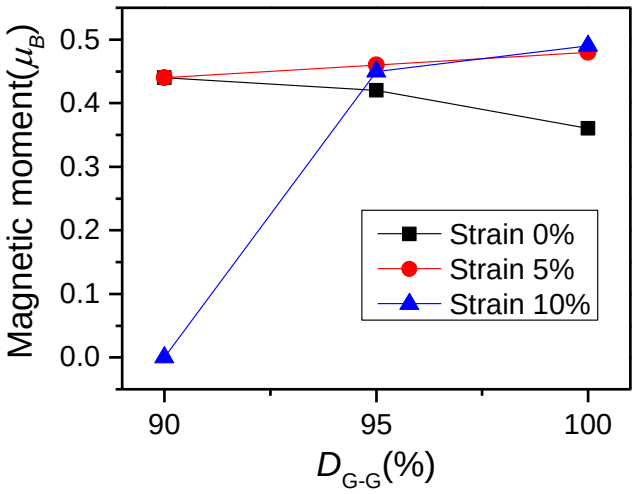

Fig. S7 The magnetic moment of $C_8Ti_3C_8$ under biaxial strains of 0%, 5%, and 10%, as a function of the distance between bilayer graphene (D_{G-G}).

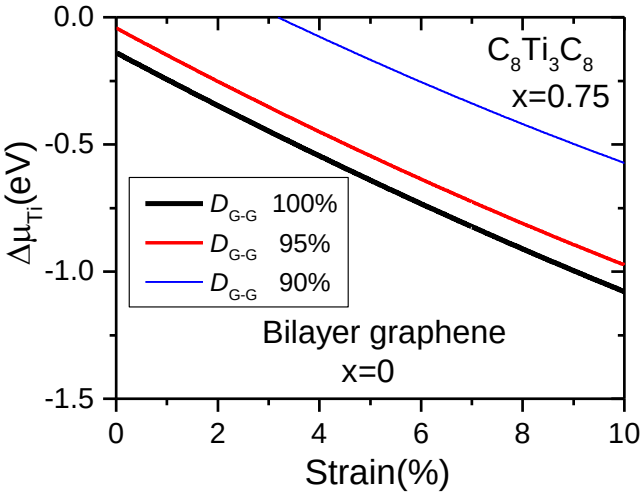

Fig. S8 The phase diagram of the most stable structures as a function of the biaxial strain and the chemical potential of Ti when considering the coverage of 0 and 0.75.

The distance between bilayer graphene, D_{G-G}, of 100% is the relaxed distance. Compressing the distance with 5%, i.e. D_{G-G} = 95%, the magnetic moments coming from the AB-TT site of $C_8Ti_3C_8$ under biaxial strains change a little, while that at the strain of 10% become 0 as further compressing the distance to 90%. Thus, the distance between bilayer graphene would affect the magnetic properties of TM-intercalated graphene. As shown in Fig. S8, when considering the Ti-intercalated BLG with the coverage of 0 and 0.75, the boundary in the phase diagram would shift up with the decrease of D_{G-G}.

D. Monaxial strain on Sc- and Ti-intercalated BLG sandwich

The phase diagram of Ti-intercalated BLG with monaxial strain applied armchair direction is almost the same as that with monaxial strain applied zigzag direction, as shown in Fig. S9. The configuration of $C_8Ti_3C_8$ is the only stable phase as monaxial strain ranging from 0% to 10%.

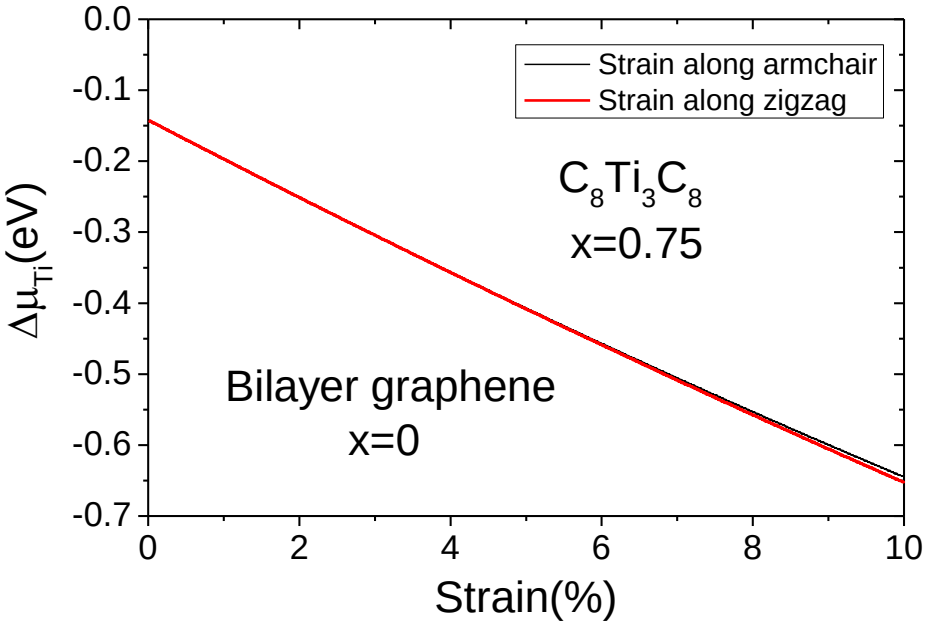

Fig. S9 The phase diagram of the most stable Ti-intercalated BLG configurations as a function of the chemical potentiaol of Ti and monaxial strain applied along armchair and zigzag directions.

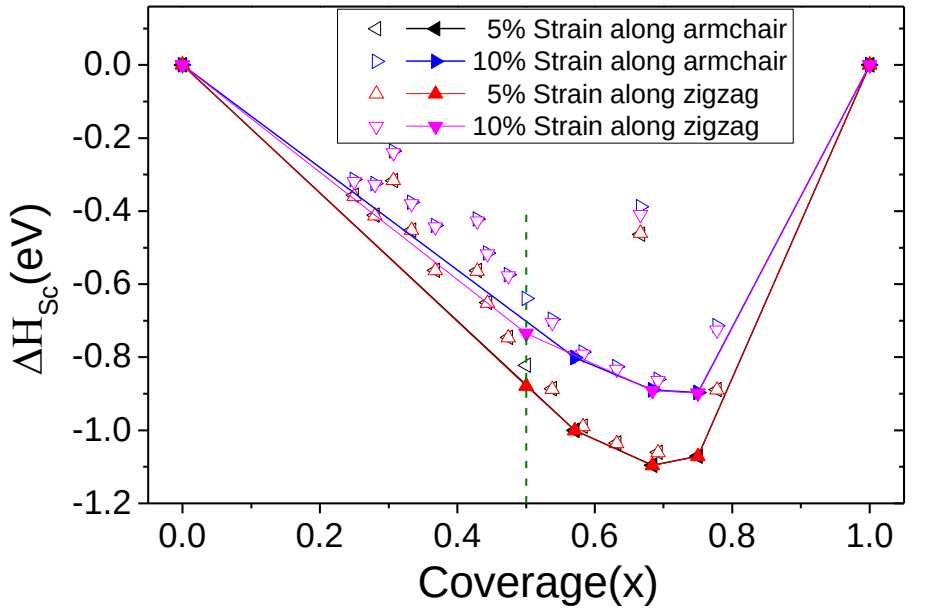

Fig. S10 The formation enthalpy for Sc-intercalated BLG as a function of coverage.

As shown in Fig. S10, the convex profile for Sc-intercalated BLG with the monaxial strain of 5% applied along armchair direction is almost the same as that along zigzag direction. The points for the coverage of 0.5 and for the strain of 5% and 10% applied along zigzag direction are convex points, while those along armchair direction stay away from the corresponding convex profiles. Thus the $C_8Sc_2C_8$ appears in the phase diagram with monaxial strain applied along zigzag direction.

References

1. J. Zhou, L. Wang, R. Qin, J. Zheng, W. N. Mei, P. A. Dowben, S. Nagase, Z. Gao and J. Lu, *J. Phys. Chem. C*, 2011, **115**, 25273-25280.